

Fission of $^{255,256}\text{Es}$, $^{255-257}\text{Fm}$, and ^{258}Md at moderate excitation energies

H. C. Britt, D. C. Hoffman, J. van der Plicht,* and J. B. Wilhelmy
Los Alamos National Laboratory, Los Alamos, New Mexico 87545

E. Cheifetz
Weizmann Institute of Science, Rehovot, Israel

R. J. Dupzyk and R. W. Lougheed
Lawrence Livermore National Laboratory, Livermore, California 94550

(Received 1 March 1984)

The fission of $^{255,256}\text{Es}$, $^{255-257}\text{Fm}$, and ^{258}Md has been studied in the excitation energy range from threshold to 25 MeV. A target of ^{254}Es was used in the direct reaction studies; (d,pf) , (t,pf) , $(^3\text{He},df)$, $(^3\text{He},pf)$, and in the compound induced fission reactions formed with p, d, t, and α particle projectiles. Coincident fission fragment energies were recorded along with (in the direct reaction studies) the outgoing light charged particle. The mass and kinetic energy distributions were studied as a function of nuclear excitation energy. The observed bulk properties were consistent with established systematics in that they exhibited an asymmetric mass distribution and a phenomenologically consistent total kinetic energy. However, the systems demonstrated a fission decay mode which we ascribe to high energy symmetric fission decay. This component, though somewhat arbitrary in its definition, showed a general decrease in yield as a function of increasing nuclear excitation energy. This observed rapid change in fission properties between "normal" and high energy symmetric fission probably points to the important observable consequences that can occur from small variations in the potential energy surface.

INTRODUCTION

The fission properties of the heavy actinides have yielded anomalous properties with regard to mass and kinetic energy distributions. A dramatic shift toward highly symmetric mass distributions accompanied with high kinetic energy release has been observed for the spontaneous fission of ^{258}Fm (Ref. 1) and ^{259}Fm .² These results differ from the extrapolation of well-known systematics which have been fitted to the lighter actinide systems.^{3,4} In contrast, the spontaneous fission of ^{259}Md (Ref. 5) has appeared to yield a mixture of fission decay properties. It gives, as do the $N \geq 158$ Fm nuclei, a symmetric mass distribution, but it has a total kinetic energy release which is substantially lower and more consistent with the phenomenological systematics derived from lighter actinides. The only other $N \geq 158$ nucleus whose fission properties have been determined is ^{256}Cf ,¹ and both the mass and kinetic energy distributions of this nucleus are more consistent with systematics observed for lighter actinides. The limited amount of data available on the fission decay properties of even higher Z (Refs. 6 and 7) nuclides (though for more neutron deficient cases) also show no apparent anomalous behavior. We have, therefore, a situation in which, for spontaneous fission, strong deviations from systematic actinide properties occur in a limited region near $Z=100$ with $N \geq 158$. Unfortunately, this region is experimentally very difficult to access unambiguously.

For the neutron-rich heavy actinides, the information on fission in excited nuclei has been limited to (n,f) studies on ^{254}Es ,⁴ ^{255}Fm ,⁸ and ^{257}Fm .⁹ For the fission of

^{256}Fm , an increase in excitation energy brought in by the neutron capture results in the observed asymmetric spontaneous fission mass distribution progressing toward a broad symmetric division.⁸ For ^{258}Fm the trend with excitation energy is to go from a highly symmetric mass distribution for spontaneous fission¹ to a distribution which, though still peaking at symmetry, shows shoulders which indicate significant yield for asymmetric division. Thus, in both ^{256}Fm and ^{258}Fm the trend is to mix symmetric and asymmetric fission with increasing excitation energy from the more pure distribution observed in spontaneous fission. To obtain more data in this interesting region and overcome the excitation energy limitations imposed by spontaneous and (n,f) studies, we have performed direct and capture reaction studies on an ^{254}Es target to expand our knowledge of heavy actinide fission properties.

EXPERIMENTAL

Access into the heavy element region was obtained via light ion reactions on an ^{254}Es target, which consisted of $\sim 0.1 \mu\text{g}$ ^{254}Es ($t_{1/2}=276$ d) deposited on a $1 \text{ mm} \times 3 \text{ mm}$ spot on a carbon foil backing. This target was prepared at the Lawrence Livermore National Laboratory isotope separator facility from enriched ^{254}Es feed material. For the direct reaction studies a beam of d, t, or ^3He was delivered from the Los Alamos FN tandem Van de Graaff. The experimental configuration is presented in Fig. 1. The charged particle direct reactions used on the ^{254}Es target were the following: $(d,p)^{255}\text{Es}^*$, $(t,p)^{256}\text{Es}^*$, $(^3\text{He},d)^{255}\text{Fm}^*$, and $(^3\text{He},p)^{256}\text{Fm}^*$. In each case the outgoing light ion was detected and identified with a $\Delta E-E$

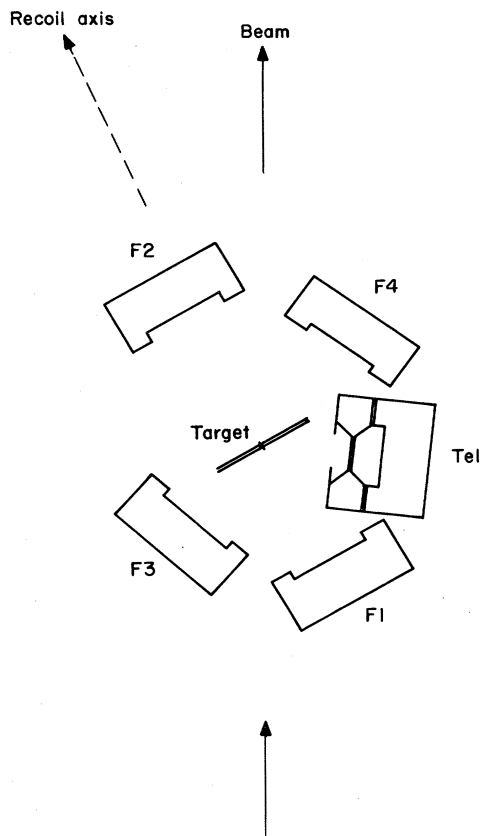


FIG. 1. Experimental configuration. Fission fragments were measured in two sets of detectors: F1–F2 or F3–F4 located at $\sim 0^\circ$ and $\sim 90^\circ$ with respect to the heavy element recoil axis.

solid state counter telescope system. The detected light ion was used to determine the excitation energy of the residual heavy isotope. The fission decay of this isotope was then measured in coincidence with the light ion by means of two sets of solid state fission detectors located at $\sim 0^\circ$ and 90° with respect to the kinematic recoil axis for the fissioning system. An Al foil was placed over the telescope to absorb the alpha particles from the radioactive decay of the target. A pile-up circuit was utilized in conjunction with the fission detectors to reject accidental α -fission summing events. The experiment had two basic objectives: (1) the measurement of the fission probabilities to extract information on the fission barriers in the heavy element region, and (2) measurement of the energetics of the fragments to obtain data on the fission mass and kinetic-energy distributions. The fission probability results have been published¹⁰ and this paper deals with the fragment energies and masses. The total number of triple coincidence events (outgoing charged particle and two fission fragments) detected were the following: (d,pf)²⁵⁵Es*–7456, (t,pf)²⁵⁶Es*–5960, (³He,d,f)²⁵⁵Fm*–4585, (³He,p,f)²⁵⁶Fm*–5088.

In addition to the direct reaction studies, a series of compound fission decays were also measured using p, d, t (11–17 MeV), and α (20–26 MeV) particles on the ²⁵⁴Es target. Since the charged particle coincidence requirement was removed, the fission counting rate was substantially

increased. In general, the measurements were performed at each particle and bombarding energy to obtain on the order of 50 000 events.

The counter telescope was calibrated via direct reactions to known levels in Pb and Zr targets. The fission detectors were calibrated according to the Schmitt, Kiker, and Williams¹¹ procedure using the pulse height spectrum of fission fragments emitted from a ²⁵²Cf source on a thin backing. In some cases, measured provisional mass and total kinetic energy (TKE) distributions were corrected to yield estimates of preneutron quantities using the Terrell¹² systematics:

$$v(A) = \begin{cases} 0.08(A - 82) & 82 \leq A \leq 122 \\ -0.26A + 34.92 & 122 < A < 132 \\ 0.1(A - 125) & 132 \leq A \leq 170 \end{cases} \quad (1)$$

with appropriate corrections for the varying E_x and TKE. The increase in the average number of neutrons emitted as a result of increased excitation energy was estimated as:

$$v_{E_x} = (E_x - E_T)A / (E_N M_F), \quad (2)$$

where v_{E_x} are the extra neutrons emitted at energy E_x , E_T is the fission threshold (taken to be 5 MeV), A is the fission fragment mass, E_N is the average energy to emit a neutron (taken to be 7.5 MeV), M_F is the mass of fissioning nucleus. The effect of kinetic energy on neutron emission was calculated from

$$v_{KE} = -[\text{TKE}(A) - \overline{\text{TKE}}(A)]A / (E_N M_F), \quad (3)$$

where $\text{TKE}(A)$ is the measured total kinetic energy for fission of a given heavy fragment mass A , and $\overline{\text{TKE}}(A)$ is the average total kinetic energy for fission of a given heavy fragment mass A [taken to be $\overline{\text{TKE}}(A) = -1.15A + 356.5$ from values extracted from Ref. 4]. The total number of neutrons emitted is the sum of Eqs. (1)–(3). From this analysis, preneutron emission mass and kinetic-energy distributions were obtained.

RESULTS AND DISCUSSION

A first test of the data is to demonstrate that credible results can be extracted from the current experimental measurements. In Fig. 2 the fragment yield, total kinetic energy, and the width of the total kinetic energy are presented as a function of heavy fission fragment mass for the excited state fission of ²⁵⁵Es. This system has been well characterized at the neutron binding energy (5.98 MeV) by Unik *et al.*⁴ via the ²⁵⁴Es(n,f) reaction ($B_f = 5.4$ MeV).¹⁰ With the ²⁵⁴Es(d,pf) reaction we have produced the same fissioning nucleus. In Fig. 2 we present our current results for an inclusive excitation energy of 4–6 MeV along with the results of Unik *et al.* Very good agreement is obtained for all mass divisions, thus giving us confidence in our basic analysis procedure.

We wish to study the fission properties as a function of excitation energy. In Fig. 3 an example is presented of the heavy fragment mass distribution for a variety of excitation energy bins for the fission of ²⁵⁵Fm produced in the ²⁵⁴Es(³He,d) reaction. At all excitation energies the distri-

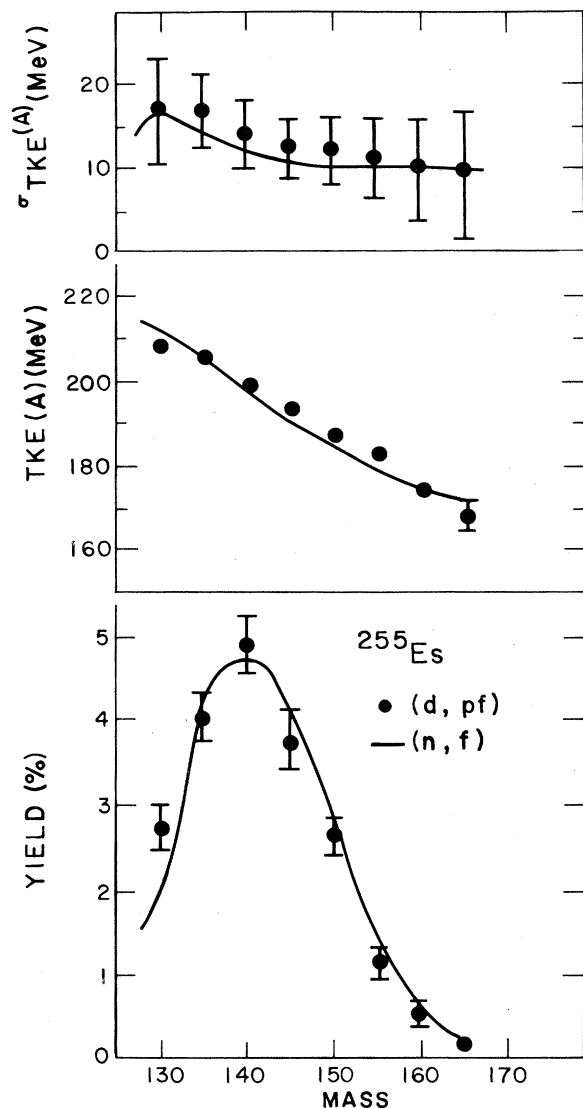


FIG. 2. Fission decay properties of $^{255}\text{Es}^*$ produced via the (n,f) reaction (Ref. 4) (solid lines) and via the current (d,pf) reaction (points) for the nuclear excitation of 4–6 MeV. The top figure shows the square root of the variance of the preneutron emission TKE, the middle figure is the preneutron emission TKE, and the bottom is the yield as a function of heavy fragment mass. The (d,pf) results were obtained after correction for neutron emission as described in the text.

butions are seen to favor an asymmetric division, though some symmetric yield is always clearly observed. In Fig. 4 a contour plot is presented for the fission of $^{255}\text{Fm}^*$ over all measured excitation energies (3–23 MeV) showing the yield as a function of total kinetic energy and heavy fragment mass. The peak yield is for an asymmetric division having a total kinetic energy release of the order of 200 MeV. However, it is quite evident that there is substantial yield of high total kinetic energy even at symmetric mass division in the ^{255}Fm fission. This high energy-symmetric component is not observed in lighter actinide fission. The occurrence of this component is presented in a more visi-

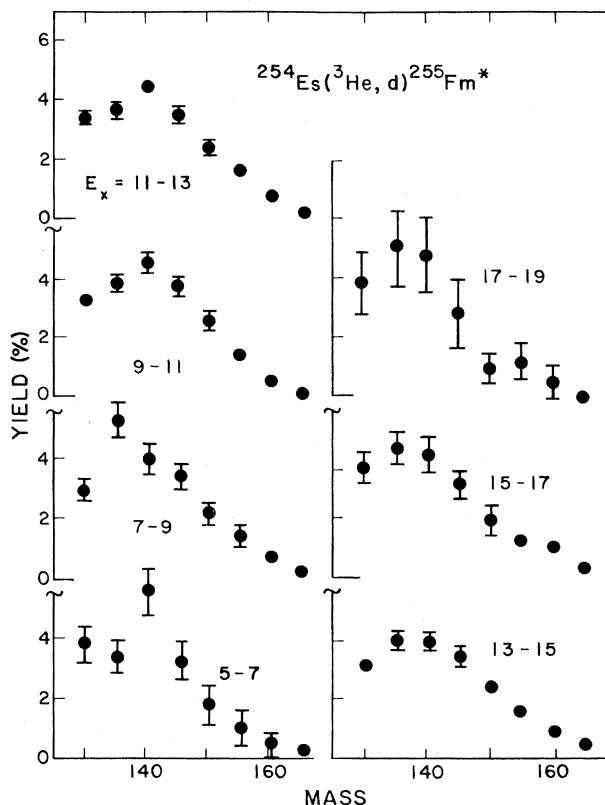


FIG. 3. Heavy fragment mass yield (preneutron emission) for various excitation energies of $^{255}\text{Fm}^*$ formed via the $^{254}\text{Es}(^3\text{He},d)^{255}\text{Fm}^*$ reaction. Neutron corrections as described in the text have been applied.

ble manner in Fig. 5 where the fragment yield is plotted as a function of total kinetic energy for $^{255}\text{Fm}^*$ summed over all measured excitation energies. Significant yield occurs even for the 240–260 MeV kinetic energy bin and it is clearly evident that the highest kinetic energy is associated with symmetric mass division. In contrast, the higher kinetic energy for lighter actinides tends to be associated with an asymmetric division.

The other measured cases show the same general properties as the above $^{255}\text{Fm}^*$ example. In no case do we observe an abrupt change from the dominant low energy asymmetric mass division to a high energy symmetric mass division as the nuclear excitation energy is increased. All cases do, however, show a contribution of high energy symmetric yield which seems to be a characteristic of fission in this heavy element region. In Fig. 6 the average total kinetic energy release is presented as a function of excitation energy for the measured cases. In order of significance, the major points to be drawn from this figure are the following: (1) the $\overline{\text{TKE}}$ values are reasonably constant for all systems at all measured excitation energies with only an $\sim 5\%$ variation between the extreme values, (2) there is a general decrease of $\overline{\text{TKE}}$ with increasing excitation energy with a slope $d(\overline{\text{TKE}})/d(E_x) \sim -0.25$ MeV/MeV, (3) with an increasing charge (and to a lesser extent, increasing neutron number) of the fissioning sys-

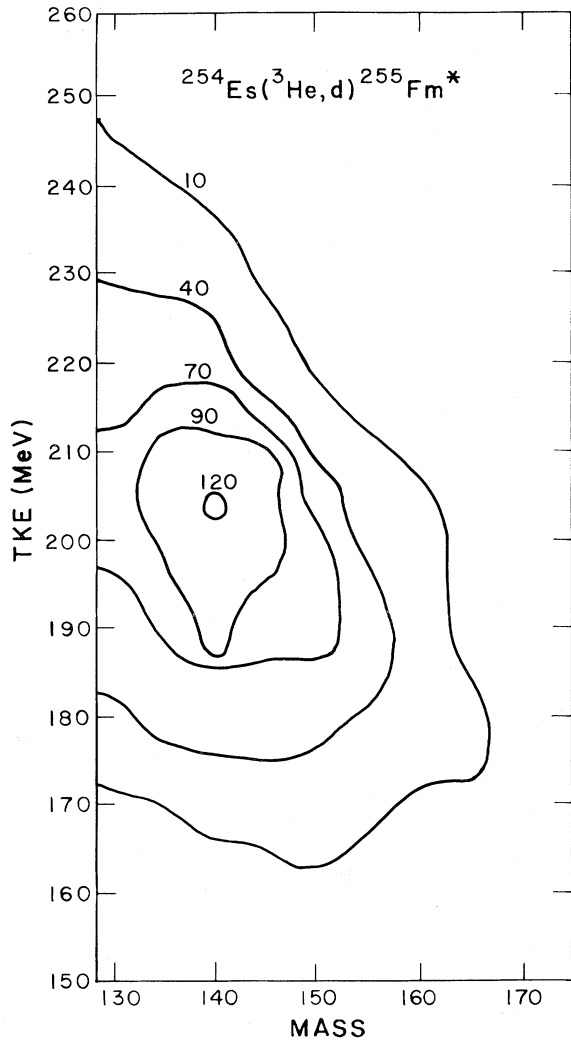


FIG. 4. Contour plot of heavy fragment yield versus preneutron emission TKE for the reaction $^{254}\text{Es}(^3\text{He},d)^{255}\text{Fm}$. The data are summed over all excitation energies (3–23 MeV). Contours are labeled by the number of observed counts. Neutron corrections as described in the text have been applied.

tem there is an increase in the $\overline{\text{TKE}}$ value for a given nuclear excitation energy. Figure 7 presents $\overline{\text{TKE}}$ vs $Z^2A^{-1/3}$ for our current data as well as that taken from the literature for other heavy actinide fission. The phenomenologically derived lines^{3,4} give a good representation of all known cases with the exception of ^{258}Fm and ^{259}Fm spontaneous fission. Though these current measurements do not show significant deviations in the average TKE, they do have, as was shown in Fig. 4, a substantial yield of “high energy symmetric fission” (HESF). To observe this distribution as a function of nuclear excitation energy we have arbitrarily chosen the definition of high energy symmetric fission to be the following: $\text{TKE} \geq 210$ MeV and $|E_1 - E_2| \leq 20$ MeV. With this definition we show in Fig. 8 the yield of HESF as a function of excitation energy for the direct reaction cases. For all cases studied the yield of this component is in the

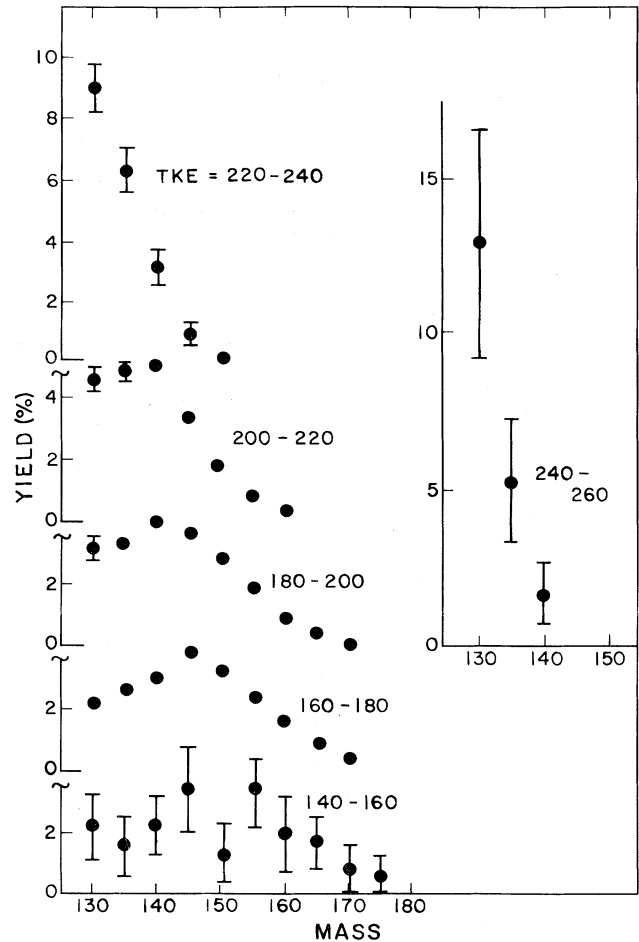


FIG. 5. Heavy fragment mass yield from the fission of ^{255}Fm produced via the $^{254}\text{Es}(^3\text{He},d)$ reaction. The data are summed over all excitation energies (3–23 MeV) and are plotted for various preneutron emission TKE regions. Neutron corrections as described in the text have been applied.

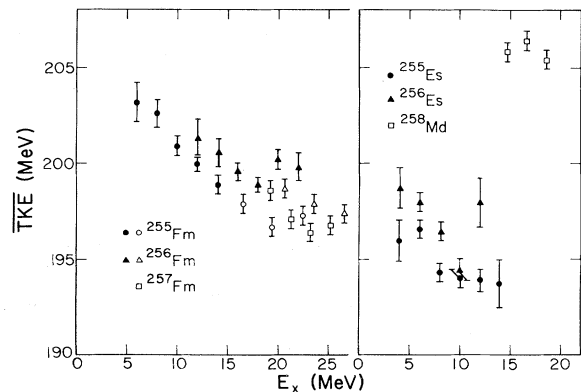


FIG. 6. Average preneutron emission TKE as a function of nuclear excitation energy for various compound nuclei. The filled symbols are for direct reaction formation and the open symbols for compound reaction formation. Neutron corrections as described in the text have been applied.

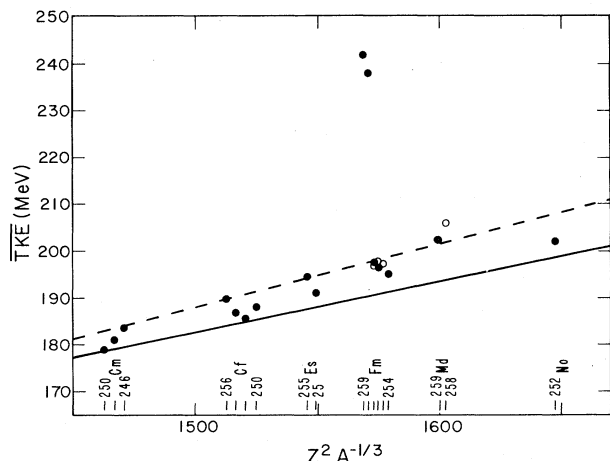


FIG. 7. Average preneutron emission TKE for a variety of heavy actinide nuclei. The systematics of Viola (Ref. 3) (solid line) and Unik *et al.* (Ref. 4) (dashed line) are also presented. The solid points are literature values (Refs. 1 and 19) and the open circles are from the current measurements.

8–24% range per fission. There is a general decrease in this yield with increasing excitation energy, but for a given excitation energy an increase in nuclear charge and neutron number results in an increased yield.

The heavy Fm region is of interest from theoretical considerations. The outer fission barrier is decreasing in magnitude and approaching a configuration which has a minimum potential energy for a symmetric shape. Analyses based on barrier properties¹³ have been able to reproduce the dramatic half-life change in the heavy Fm isotopes by predicting that the outer fission barrier has fallen below the ground state energy. This causes an abrupt decrease in the tunneling requirement and a corresponding decrease in the spontaneous fission half-life. These calculations predict the change should occur between ^{258}Fm and ^{260}Fm while in the experimental data¹⁴ the abrupt change occurs between ^{256}Fm – ^{258}Fm (a change in half-life by a factor of 3×10^{-8}). The fission mass distribution properties may also be influenced by the rapidly decreasing outer barrier and its trend toward a mass symmetric shape. Analysis based on the mass distribution being

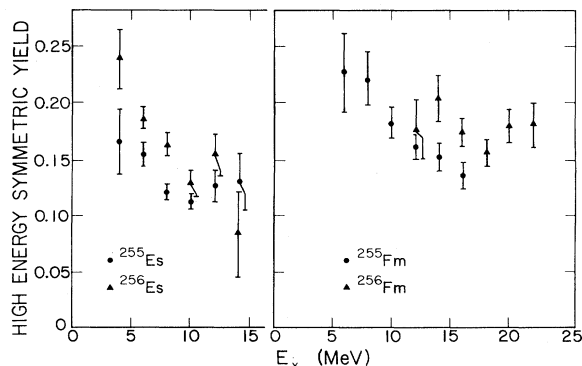


FIG. 8. High energy symmetric fission yield (see the text) as a function of excitation energy for the indicated systems.

determined by saddle point properties¹⁵ has been moderately successful in predicting trends. However, the more quantitatively successful models have been based on an asymmetric two center shell model analysis¹⁶ and on a scission point model¹⁷ based on the potential energy surface near the scission configuration. These models have demonstrated that the shell effects in the forming fragments play an important role in determining fission observables. It is an interesting coincidence that analyses based on either barrier properties or those on fragment shells are indicating rapidly changing effects in the heavy Fm region. Most of the predictions are for spontaneous fission properties. The general trend is that the shell effect will become less important as excitation energy is

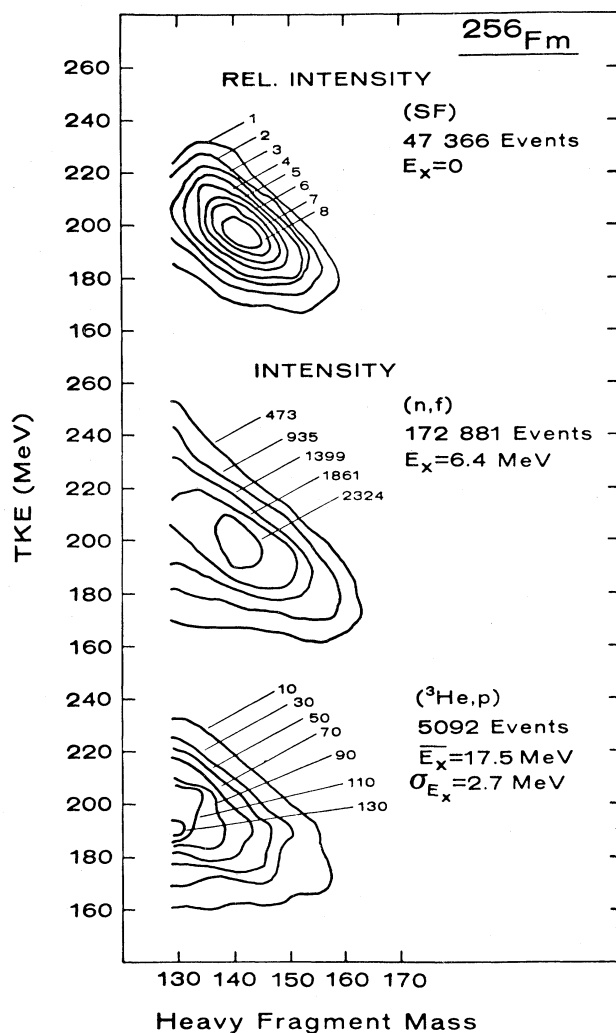


FIG. 9. Contour plots of heavy fragment yield versus TKE for the fission of ^{256}Fm . The top figure is for the preneutron emission masses and kinetic energies for the spontaneous fission decay and is taken from Ref. 18. The middle figure is for $^{255}\text{Fm}(n_{\text{th}},f)$ taken from Ref. 8 and is for provisional masses and kinetic energies. The bottom figure is for the $^{25}\text{Es}(^3\text{He},p)$ reaction summed over all measured excitation energy ($E_x = 17.5$ MeV, $\sigma_{E_x} = 2.7$ MeV) for provisional masses and total kinetic energy.

added to the fissioning system. Our observations imply that we have a mixture of fission modes in all the heavy element cases studied.

In Fig. 9 we present contour diagrams of yield versus TKE and heavy fragment mass for ^{256}Fm at three different excitation energies. The spontaneous fission results show an asymmetric system whose bulk properties are well reproduced by fission phenomenology. However, even for this case there is an indication of a large variance in the TKE release near symmetric division. As the excitation energy is increased to the (n_{th}, f) region, an increase in yield for symmetric division is observed. Also, there is now significant yield in the high energy symmetric fission region. As the excitation energy is increased further via the $^{254}\text{Es}(^3\text{He}, p)^{256}\text{Fm}$ reaction we observe a continued evolution of the system. Now the mass yield has become symmetric and broad. However, the TKE distribution, though being broad, no longer seems to have a distinct tendency toward a two component distribution. The high energy symmetric fission yield is not readily discernable under these conditions. For the ^{256}Fm nucleus the increasing excitation energy first increases the HESF yield, but then this effect is washed out at yet higher energies. This change with excitation energy may be pointing to the importance of shell effects in the potential energy surface for determining fission properties. As presented by Mustafa and Ferguson,¹⁶ the preference for asymmetry is very slight in the ^{256}Fm system at the deformation they considered (the neck radius, $D=4$ fm). With the ~ 6 MeV of excitation energy brought in through neutron capture the system would be expected to sample the symmetric distribution with some appreciable yield. However, population in the symmetric component at this specific deformation cannot ensure that there will be appreciable yield for final symmetric division as the system evolves toward fission. The dynamical effects associated with the movement toward scission could provide substantial variation from the

adiabatic conditions implied by the potential energy surface analysis. The observed high TKE associated with some of the symmetric yield, points toward a more compact scission configuration for these decays. Our observations would be more consistent with a distinct potential energy minimum nearer the scission configuration. The subsequent disappearance of the observed HESF at the energies reached with the $(^3\text{He}, p)$ reaction would also be more consistent with a scission analysis where the increasing intrinsic temperature results in a washing out of the shell effects¹⁷ and an eventual broad symmetric fragment mass distribution.

In Fig. 10 the spontaneous and (n, f) induced fission for ^{256}Fm and ^{258}Fm are presented. The spontaneous fission distributions for the two nuclei are strikingly different. The ^{256}Fm is a fairly normal asymmetric division with TKE consistent with the phenomenological systematics. The $^{258}\text{Fm}(\text{SF})$ is (with relatively poor experimental statistics²) completely associated with HESF. However, $^{256}\text{Fm}^*$ and $^{258}\text{Fm}^*$ at the excitation energy reached following thermal neutron capture now show a much more similar mass-yield distribution. Both have components of "normal" fission and the HESF. We feel these results point toward the importance of small differences in the potential energy surface leading to major changes in the fission observables. Clearly the heavy Fm region is a transition area where competing fission modes can have substantial yields. Though these observed properties are not predicted in detail by the Wilkins, Steinberg, and Chasman¹⁷ model they are in the general spirit of their analysis. The region of the potential energy surface that decides the yield of the fission observables apparently has shallow minima separating asymmetric and symmetric divisions. In the case of ^{256}Fm the asymmetric minimum must be deeper and for ^{258}Fm the symmetric minimum should dominate. With modest increase of energy (the neutron binding energy) both systems sample the two valleys. With yet higher energies (for the studied ^{256}Fm case) the shallow minima are overcome by the intrinsic excitation energy resulting in a damping of the shell effects and the system reverts toward a broad symmetric fission distribution.

CONCLUSIONS

The neutron-rich region in the vicinity of $Z=100$ shows striking fission behavior. We have studied the effect of nuclear excitation energy on the fissioning nuclei $^{255,256}\text{Es}$, $^{255-257}\text{Fm}$, and ^{258}Md using direct and compound nuclear reactions. The overall mass distributions were found to be predominately asymmetric and the TKE release consistent with established phenomenological models. There is a general decrease of TKE as a function of increasing nuclear excitation energy. However, the most significant observation is that for the studied cases there is a fission component which we have assigned to high energy symmetric fission. Though it is not possible to define this component unambiguously, we have chosen, as a working definition, the conditions $|E_1 - E_2| \leq 20$ MeV and $\text{TKE} \geq 210$ MeV. With this definition the HESF component varied between 8–24% of the total yield. There is a general decrease of this component with

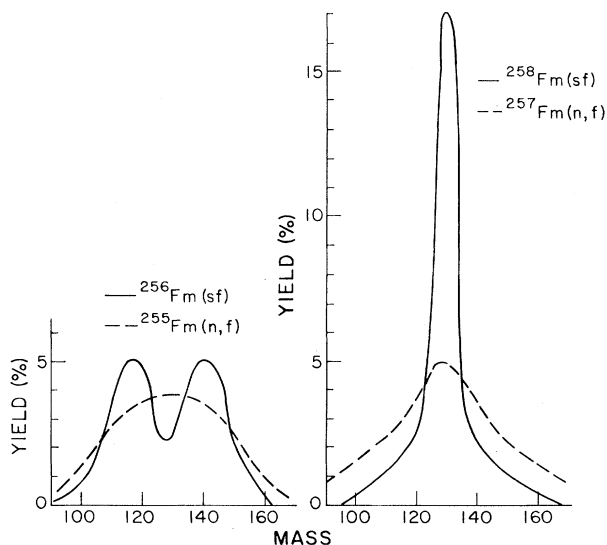


FIG. 10. Provisional mass distributions (no neutron corrections) for $^{256}\text{Fm}(\text{SF})$ (Ref. 1), $^{255}\text{Fm}(n, f)$ (Ref. 8), $^{258}\text{Fm}(\text{SF})$ (Ref. 2), and $^{257}\text{Fm}(n, f)$ (Ref. 9).

increasing nuclear excitation energy. Combining our data with previous studies we observe that, at the neutron capture excitation energy, ^{256}Fm and ^{258}Fm both have broadly symmetric mass divisions that are qualitatively similar. However, the spontaneous fission distributions of these two isotopes are markedly different with the $^{256}\text{Fm}(\text{SF})$ being "normally" asymmetric while the $^{258}\text{Fm}(\text{SF})$ is highly symmetric. These systematics may point toward the importance of the influence of small shell stabilized perturbations on the potential energy surface leading toward fission. These observations are most consistent with the gross properties of the scission point model of Wilkins, Steinberg, and Chasman.¹⁷ The possibility of thus determining fission properties from a potential energy sur-

face analysis very near the scission configuration shows the inherent adiabatic character of the process and limits the intrinsic excitation that can be put into the system by viscous dissipation of the flowing nuclear matter.

ACKNOWLEDGMENTS

We wish to thank the Transplutonium Production Program of the U.S. Department of Energy (DOE) for supplying the ^{254}Es target material. The expert assistance of the personnel of the Los Alamos Van de Graaff facility is appreciated. This work was performed under the auspices of the U.S. DOE.

*Present address: National Superconducting Cyclotron Laboratory, Michigan State University, East Lansing, MI 48824.

- ¹D. C. Hoffman, J. B. Wilhelmy, J. Weber, W. R. Daniels, E. K. Hulet, R. W. Lougheed, J. H. Landrum, J. F. Wild, and R. J. Dupzyk, *Phys. Rev. C* **21**, 972 (1980).
²E. K. Hulet, R. W. Lougheed, J. H. Landrum, J. F. Wild, D. C. Hoffman, J. Weber, and J. B. Wilhelmy, *Phys. Rev. C* **21**, 966 (1980).
³V. E. Viola, *Nucl. Data Sect. A* **1**, 391 (1966).
⁴J. P. Unik, J. E. Gindler, L. E. Glendenin, K. F. Flynn, A. Gorski, and R. K. Sjoblom, in *Proceedings of the Third International Atomic Energy Agency Symposium on the Physics and Chemistry of Fission, 1973* (International Atomic Energy Agency, Vienna, 1974), Vol. II, p. 19.
⁵J. F. Wild, E. K. Hulet, R. W. Lougheed, P. A. Baisden, J. F. Landrum, R. J. Dougan, M. G. Mustafa, *Phys. Rev. C* **26**, 1531 (1982).
⁶C. E. Bemis, Jr., R. L. Ferguson, F. Plasil, R. J. Silva, F. Pleasonton, and R. L. Hahn, *Phys. Rev. C* **15**, 705 (1977).
⁷C. E. Bemis, Jr., R. L. Ferguson, F. Plasil, R. J. Silva, G. D. O'Kelley, M. L. Kiefer, R. L. Hahn, D. C. Hensely, E. K. Hulet, and R. W. Lougheed, *Phys. Rev. Lett.* **39**, 1246 (1977).
⁸R. C. Ragaini, E. K. Hulet, R. W. Lougheed, and J. Wild,

Phys. Rev. C **9**, 399 (1974).

- ⁹W. John, E. K. Hulet, R. W. Lougheed, and J. J. Wesolowski, *Phys. Rev. Lett.* **27**, 45 (1971).
¹⁰H. C. Britt, E. Cheifetz, D. C. Hoffman, J. B. Wilhelmy, R. J. Dupzyk, and R. W. Lougheed, *Phys. Rev. C* **21**, 761 (1980).
¹¹H. W. Schmitt, W. E. Kiker, and C. W. Williams, *Phys. Rev.* **137**, B837 (1965).
¹²J. Terrell, *Phys. Rev.* **127**, 880 (1962).
¹³J. Randrup, C. F. Tsang, P. Möller, and S. G. Nilsson, *Nucl. Phys. A* **217**, 221 (1973).
¹⁴E. K. Hulet, J. F. Wild, R. W. Lougheed, J. E. Evans, B. J. Qualheim, M. Nurmia, and A. Ghiorso, *Phys. Rev. Lett.* **26**, 523 (1971).
¹⁵C. F. Tsang and J. B. Wilhelmy, *Nucl. Phys. A* **184**, 407 (1972).
¹⁶M. G. Mustafa and R. L. Ferguson, *Phys. Rev. C* **18**, 301 (1978).
¹⁷B. D. Wilkins, E. P. Steinberg, and R. R. Chasman, *Phys. Rev. C* **14**, 1832 (1976).
¹⁸D. C. Hoffman, G. P. Ford, J. P. Balagna, and L. R. Veaser, *Phys. Rev. C* **21**, 637 (1980).
¹⁹D. C. Hoffman and M. M. Hoffman, *Annu. Rev. Nucl. Sci.* **24**, 151 (1974).